Correspondence Preserving Elastic Surface Registration with Shape Model Prior

F. Danckaers*, T. Huysmans*, D. Lacko*, A. Ledda, S. Verwulgen†, S. Van Dongen‡ and J. Sijbers*
*iMinds Vision Lab, dept. of physics, University of Antwerp. Email: {femke.danckaers, toon.huysmans, daniel.lacko, jan.sijbers}@uantwerp.be
†Faculty of Design Sciences, University of Antwerp. Email: stijn.verwulgen@uantwerp.be
‡Group of Evolutionary Biology, dept. of biology, University of Antwerp. Email: stefan.vandongen@uantwerp.be

***Abstract*—In this paper, we describe a framework for surface registration. The framework consists of a combination of rigid registration, elasticity modulated registration and the use of a shape model prior. The main goal in this paper is to minimize the geometric surface registration error while maintaining correspondences. Experiments show improved geometric fit, correspondence, and timing compared to the current state of the art. Possible applications of the framework are construction of correspondences for shape models, reconstruction of missing parts, and artifact reduction.**

I. Introduction

Surface registration is a frequently used technique in many applications, such as surface recognition [1], [2] or surface reconstruction [3], [4]. The goal of surface registration is to deform one surface to another while finding a meaningful mapping between the vertices of the surfaces, by maintaining the correspondences. The distance between corresponding points on the target surface and the deformed source surface must be minimal.

A developer of products that have to fit closely to the human body or a part of it, needs to gain insight into the shape variability of that specific part of the body of a target population. Statistical shape modeling is a promising approach to map out this variability [5]. The construction of such models, based on surface-to-surface correspondences is, however, a challenging task. 3D surface registration is an elegant approach to obtain such correspondences. Based on the distribution of the shape variances, ergonomic products can be developed and tested on characteristic shapes. Furthermore, shape models are useful in intelligent systems for made-to-measure products [6].

Obtaining surface correspondences can be done manually [7], but this is time-consuming and error prone. The current challenges for surface registration are flexibility, robustness and performance [5]. Surface registration can be done by parametrization [8]–[11]. A mapping between the source and target surface is obtained through parameterization to a common mathematical domain, such as a sphere or cylinder. The disadvantage of such a technique is that the surfaces must have the same non-complex topology, because they have to be deformed to the same target space.

Another approach is spatial registration, where features are matched [1], [12], [13]. With these techniques, each vertex is transformed individually. Amberg et al. [14] presented an algorithm in which each vertex is displaced separately by an affine transformation matrix, but with constraints. They introduced a stiffness, causing a vertex to be displaced along with its neighbors. The stiffness value decreases during the iterations, allowing a more elastic deformation. This results in a good geometric fit, but often poor correspondences.

Our main goal was to develop a registration framework that provides an accurate geometric fit while maintaining correspondences. In this paper, a method for surface registration with automatic transfer of correspondences from the source to the target surface is described. The proposed framework extends Amberg's approach by splitting the registration step into a local and global part and by exploiting prior knowledge i.e. a shape model [15] in elastic surface registration. The shape model has the advantage that realistic deviations of the mean are known. The combination with elasticity makes the framework more flexible and a better geometric fit is obtained with improved correspondences.

II. Method

In this section, the developed framework is described. It extends the elegant algorithm of Amberg [14] by separating the global registration from the local registration step and adding a shape model prior, resulting in a more efficient algorithm. The framework is illustrated in Fig. 1.

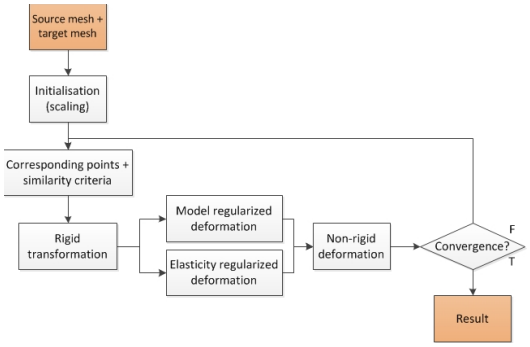

Fig. 1: The framework of the proposed algorithm.

The surfaces are represented by triangle meshes and no landmark information is used. The algorithm is however trivially extendible to include prior landmark correspondences cfr. Amberg.

1051-4651/14 $31.00 © 2014 IEEE
DOI 10.1109/ICPR.2014.373

A. Amberg

1) N-ICP-A: In [14], Amberg et al. presented the nonrigid optimal step iterative closest points (ICP) algorithm with affine transformation matrices (N-ICP-A). Each vertex undergoes a transformation, while motion is restricted by a stiffness factor β that regulates the strength of the connection with the neighboring vertices and which decreases during the iterations. In this way, the movement of neighboring vertices is constrained, resulting in similar movements for nearby vertices, as displayed in Fig. 2. This affine transformation matrix implies also a global alignment.

By applying weights to each vertex, the importance of this vertex can be set. When there is no corresponding point found for a vertex of the target mesh, its weight is set to zero. In that case, this vertex simply translates along with its neighboring vertices. While many weighting schemes are possible, we used binary weights for simplicity, which were observed to be sufficient.

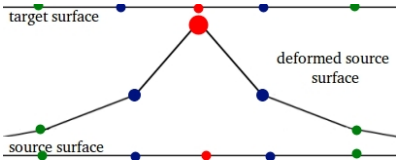

Fig. 2: Schematic representation of elasticity. If one vertex, in this case the red dot, is transformed, the neighboring vertices are forced to move along with this vertex. The closest neighbors (blue dots) are the stiffest and move more than the distant neighbors (green dots).

Let $\mathbf{X}$ be a $3n_v \times 4$ matrix that stores a 3×4 affine transformation matrix for each vertex of the source surface. $\mathbf{X}$ can be determined by solving a linear system that consists of three expressions.

- The stiffness term $E_s(\mathbf{X})$ is the Frobenius norm $||\cdot||_F$ of the Kronecker product $\otimes$ of incidence matrix $\mathbf{M}$ and matrix $\mathbf{G}$. $\mathbf{M}$ is a $n_e \times n_v$ matrix, with n_e the number of edges and n_v the number of vertices. $\mathbf{M}$ indicates the start (-1) and end (+1) vertex of each edge. $\mathbf{G}$ is a diagonal matrix $diag(1, 1, 1, 1)$. Hence:

$$E_s(\mathbf{X}) = ||(\mathbf{M} \otimes \mathbf{G})\mathbf{X}||_F^2 \tag{1}$$

- The distance term $E_d(\mathbf{X})$ is built up from a $n_v \times n_v$ diagonal weight matrix $\mathbf{W}$, which indicates the weight of each vertex. Let $\mathbf{V}$ be a sparse $n_v \times 4n_v$ matrix that holds the coordinate vectors $\mathbf{v}$ of the source surface, with $\mathbf{v}_i = [x\, y\, z\, 1]^T$, where $\mathbf{v}_i$ starts at position $(i, 4i)$ of $\mathbf{V}$. Furthermore, $n_v \times 3$ matrix $\mathbf{T}$ holds the coordinates of the corresponding point for each vertex on the target surface. Then,

$$E_d(\mathbf{X}) = ||\mathbf{W}(\mathbf{V}\mathbf{X} - \mathbf{T})||_F^2 \tag{2}$$

- The landmark term $E_l(\mathbf{X})$ consists of $n_v \times 3$ matrix $\mathbf{T}_L$ and $n_v \times 4n_v$ matrix $\mathbf{S}_L$, which are the landmark matrices.

$$E_l(\mathbf{X}) = ||\mathbf{S}_L\mathbf{X} - \mathbf{T}_L||_F^2 \tag{3}$$

The sum of the terms must be minimized. All terms together give a system that must be solved for $\mathbf{X}$:

$$\begin{bmatrix} \beta\mathbf{M} \otimes \mathbf{G} \\ \mathbf{WV} \\ \gamma\mathbf{S}_L \end{bmatrix} \mathbf{X} = \begin{bmatrix} \mathbf{0} \\ \mathbf{WT} \\ \mathbf{T}_L \end{bmatrix} \tag{4}$$

In Eq. (4), β represents the stiffness factor that limits the deformation and γ is the landmark weight, used to control the importance of the landmarks. Landmarks are, however, not used in this paper.

2) N-ICP-T: In the nonrigid optimal step ICP algorithm with transformation vertices (N-ICP-T) of Amberg et al. [14], the vertices are only allowed to translate. This is a simplified version of the N-ICP-A method and results in larger geometric and correspondence errors, as rotation of the object is not possible. The $\mathbf{W}(\mathbf{T}-\mathbf{S})$ matrix is a $n_v \times 3$ matrix and represents the weighted distances between each vertex on the source surface $\mathbf{S}$ and its corresponding point on the target surface $\mathbf{T}$

$$\begin{bmatrix} \beta\mathbf{M} \\ \mathbf{WI} \end{bmatrix} \mathbf{X} = \begin{bmatrix} \mathbf{0} \\ \mathbf{W}(\mathbf{T} - \mathbf{S}) \end{bmatrix} \tag{5}$$

Eq. (5) must be solved for $\mathbf{X}$, which is a $n_v \times 3$ matrix of displacement vectors. Each row represents the translation vector for its associated vertex.

B. Registration of Two Surfaces

For the first part of our framework, in order to obtain a population correspondence, one surface of the population is registered to every other surface of the population. By this step, the points of the source surface will be located on the same anatomical locations on the deformed source surface. Both surfaces are defined as triangular meshes.

First, a rigid registration is performed. The next part of the registration procedure is done by iteratively repeating a rigid registration combined with an elasticity modulated registration.

$$\mathbf{S}_i = (1 - \alpha) \cdot R(\mathbf{T}, \mathbf{S}_{i-1}) + \alpha \cdot E(\mathbf{T}, \mathbf{S}_{i-1}, \beta) \tag{6}$$

In Eq. (6), $\mathbf{S}_i$ is the $n_v \times 3$ matrix that contains the coordinates of the vertices of the source surface at iteration i. Furthermore, $R(.)$ and $E(.)$ represent the rigid and elastic registration, respectively.

The combination of both techniques is balanced with a weight factor $\alpha \in [0, 1]$. At the first stage of the registration, the rigid registration is more important. Later, the elastic registration becomes more apparent.

During the iterations, α will increase and β will decrease. This makes that the elastic deformations will become more prominent with respect to the rigid transformation through the iterations. β is updated every u iterations.

$$u = \frac{N}{\beta_{start} - \beta_{end}} \tag{7}$$

with N the total number of iterations. β is determined by

$$\beta_i = \beta_{i-1} - \left(\frac{\beta_{start} - \beta_{end}}{N} \right)^2 \tag{8}$$

Appropriate values for these weights have been obtained empirically. For this paper, α goes from 1 to 0 and β goes from 50 to 5. In Section III-E, the influence of the stiffness term is investigated.

We will refer to the above algorithm as RN-ICP-T, because it combines a rigid registration and the N-ICP-T algorithm of Amberg. In the following subsection, the RN-ICP-T algorithm is discussed in more detail.

1) Rigid Registration: By this step, a rigid transformation is performed. First, in both surfaces corresponding points are identified. This is done by casting a ray along the normal $\mathbf{n}_s$ of a vertex of the source surface to the target surface. The intersection point does not have to be a vertex, but can be any location on the target surface. The direction of the normal $\mathbf{n}_t$ of this intersection point of the ray with the target surface is compared with the direction of $\mathbf{n}_s$ by

$$d = \mathbf{n}_s \cdot \mathbf{n}_t \tag{9}$$

If the dot product $d > 0.5$, the points can be considered as corresponding points. Multiple intersections of the normal ray with the target surface are possible. The vertices with normals for which $d > 0.5$ and at the shortest Euclidean distance from each other, are corresponding points. The second constraint is that two points can only be corresponding if the line segment between them does not intersect the surface. The corresponding points are mapped onto each other to find the optimal affine transformation matrix for the surface, by least-squares minimization. This means that the distance between corresponding points is minimal.

2) Elasticity Modulated Registration: Apart from a global transformation, also local deformations are needed to obtain an accurate geometric fit. It is implemented by using the N-ICP-T formula of Amberg's algorithm, which minimizes the difference between the translations of neighboring vertices. We chose for the N-ICP-T algorithm because it has four times less linear equations than the N-ICP-A algorithm, what leads to a much shorter calculation time for solving the linear system. In combination with a rigid transform, N-ICP-T even gives an improved geometric fit and a smaller correspondence error regarding to the current state of the art.

C. Building a Shape Model

The second part of our framework consists of building a statistical shape model [8] based on the correspondences that resulted from the surface registration. This is done by using principal components analysis (PCA). In this model, the mean surface and the eigenmodes are incorporated. To build a shape model using PCA, it is important that the surfaces are superimposed by optimally translating and rotating the surfaces The optimal poses are determined by Procrustes analysis. A shape model can be presented with following formula.

$$\mathbf{y} = \mathbf{C}(\bar{\mathbf{X}} + \boldsymbol{\Phi}\mathbf{b}) \tag{10}$$

In Eq. (10), $\mathbf{y}$ denotes an instance of the model, $\bar{\mathbf{X}}$ represents the mean surface, $\mathbf{C}$ is a similarity transformation and $\mathbf{b}$ are the shape parameters. The matrix that holds the eigenvectors of the shape model is represented by $\boldsymbol{\Phi}$. This means that a new, realistic surface can be formed by adapting the shape model parameters.

D. Surface Registration with Shape Model Prior

In this section, the approach for registration with a shape model prior is discussed. A shape model contains more information than a single surface, so it is expected that this will give improved correspondences than registration starting from a single surface. The goal is to minimize the distance between the corresponding points, by deforming the shape model in combination with a further elastic deformation.

Surface registration with a shape model is done by combining a model regularized registration with an elasticity regularized registration to obtain good results on both geometric fit and correspondences. The elasticity regularized registration is the same as described before in Section II-B2, but the model regularized registration requires a different approach because the model variances are incorporated.

We will refer to the above algorithm by RNM-ICP-T. This algorithm is similar to the RN-ICP-T algorithm, but makes use of prior shape model knowledge instead of registration with a random source surface.

1) Model Regularized Registration: First, a fitting of the PCA model to the target surface is done, effectively deriving the contributions for each of the shape modes. The goal is to adjust the principal component contributions so that the model approaches the shape of the target surface. The number of shape modes m that are included in each iteration i are calculated by following formula.

$$m_i = ceil(\frac{m_{i-1}}{4} \cdot \frac{4 \cdot (i+1)}{N}) \tag{11}$$

where N stands for the total number of iterations. m_0 is the total number of shape modes of the shape model.

The model parameters $\mathbf{b}$ can be found by solving

$$\boldsymbol{\Phi}_{m_i}^T \cdot \mathbf{W}\boldsymbol{\Phi}_{m_i} \cdot \mathbf{b} = \boldsymbol{\Phi}_{m_i}^T \cdot \mathbf{W}(\mathbf{t} - \bar{\mathbf{s}}) \tag{12}$$

In Eq. (12), $\mathbf{W}$ is a diagonal $3n_v \times 3n_v$ matrix that holds the weights, $\mathbf{t}$ is the vector that holds the positions of the vertices of the target mesh and $\bar{\mathbf{s}}$ the vector holds the positions of the mean mesh, both with size $3n_v$. Matrix $\boldsymbol{\Phi}m_i$ is a $3n_v \times n_m$ matrix that holds the first m_i shape modes. A new surface is formed by the mean shape and a linear combination of the principal components, with parameters $\mathbf{b}$.

The algorithm for registration with a shape model is a combination of both model regularized registration M and elasticity regularized registration E.

$$\mathbf{S}_i = (1-\alpha) \cdot M(\mathbf{T}, \mathbf{S}_{i-1}) + \alpha \cdot E(\mathbf{T}, \mathbf{S}_{i-1}, \beta) \tag{13}$$

III. Evaluation

In this section, the results of the performed tests are described. Due to the large calculation time, only the results of the human head registration are compared with the N-ICP-A algorithm of Amberg. The framework is tested on the full body and specific body parts. Each registration technique is set to

run for a minimum of 50 iterations and a maximum of twice the set number of iterations or when convergence is obtained. This is when the convergence ratio c is less than 0.0001. The calculation is based on the current (i) and previous $(i-1)$ mean distance d between the source and target surface.

$$c = \frac{d_i - d_{i-1}}{d_i} \tag{14}$$

In Section III-C, tests are performed on the quality of the geometric fit, in Section III-D the quality of the correspondences and in Section III-F the execution time of the algorithm. The influence of the stiffness term and number of iterations are also tested in resp. Section III-E and Section III-G.

A. Data Sets

For the performed tests, four classes of data sets are used. There are 106 full-body scans, 150 ear scans, 90 clavicula scans, and 100 head scans.

B. Shape Model

For this illustration, a shape model is built from 100 MRI scans of human heads, that are registered with one surface. The five first shape modes of the model are displayed in Fig. 3.

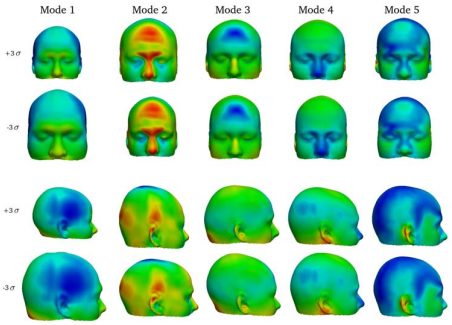

Fig. 3: The first five eigenmodes of the head model, plus and minus 3 standard deviations. The model is created from 100 surfaces. The colors indicate the magnitude of the landmark covariance tensor from blue (little variation) to red (many variation).

C. Evaluation of the Geometric Fit

It is important that the registration results in an accurate geometric fit. This means that the distance between the deformed source surface and the target surface must be minimal.

In Table I, the error on the geometric fit (in mm) from the deformed target surface on the source surface are summarized. There, the distance from each point of the deformed source mesh is measured to the closest point on the target mesh.

	N-ICP-A	**RN-ICP-T**	**RNM-ICP-T**
head	0.022 ± 0.006	0.006 ± 0.007	**0.006 ± 0.001**
body	-	0.092 ± 0.072	**0.053 ± 0.040**
ear	-	0.346 ± 0.334	**0.095 ± 0.067**
clavicula	-	0.065 ± 0.007	**0.052 ± 0.005**

TABLE I: Geometric error (mm).

It can be seen that the proposed algorithms result in an improved geometric fit compared to the N-ICP-A algorithm.

D. Evaluation of the Correspondence Quality

For evaluating the correspondences, some characteristic points are annotated on the source mesh. The same anatomical locations are annotated on the target mesh. When the registration is done, these locations can be loaded again on the deformed mesh. The Euclidean distance between corresponding points in the target mesh and deformed source mesh is calculated. The smaller this distance, the better. In Figure 4, the validation of the correspondences is shown for a typical surface.

With N-ICP-A, the vertices are deformed to the closest point without aligning the surface features properly. While it leads to negligible geometric errors, the correspondence error is generally large. This is clearly visible in the shoulder area in Fig. 4e. When using a shape model, the surfaces are globally well registered before local deformations are allowed.

In Table II the results of the tests are shown. The algorithm is performed on 10 surfaces of each class. The mean correspondence error (in mm) is displayed in the table.

	N-ICP-A	**RN-ICP-T**	**RNM-ICP-T**
head	6.13 ± 1.16	4.23 ± 0.89	**4.14 ± 0.89**
body	-	26.84 ± 3.61	**25.88 ± 3.35**
ear	-	4.09 ± 2.75	**2.18 ± 0.51**
clavicula	-	**4.42 ± 1.33**	4.50 ± 1.36

TABLE II: correspondence error (mm)

The N-ICP-A algorithm of Amberg gives significantly larger errors. This is because there is no overall rigid allignment step, so the chances are higher that the source vertices migrate to a wrong position on the target vertex. Once such an error is made, the algorithm is not capable of repairing this. The proposed technique makes use of a separate, overall rigid step and also a global non-rigid registration by the shape model, which makes the registration more robust.

Evidenced by the results, the RN-ICP-T and RNM-ICP-T algorhithms give the smallest errors. The results of the RNM-ICP-T algorithm are the most stable. It is clear that the algorithm of Amberg gives the worst results on correspondence.

E. Evaluation of the Sensitivity of the stiffness

For this test, the stiffness value evolves from 50 to 5. This value is empirically determined. The smaller the stiffness value, the more freely the vertices can move.

The influence of the stiffness depends on the number of triangles on the surface. The more triangles, the smaller the distance between neighboring points. This means that a surface with many triangles will be less elastic than a surface with less triangles. When a surface is highly curved, finding corresponding points will be more difficult and it is less likely that all corresponding points can be found. In that case it is

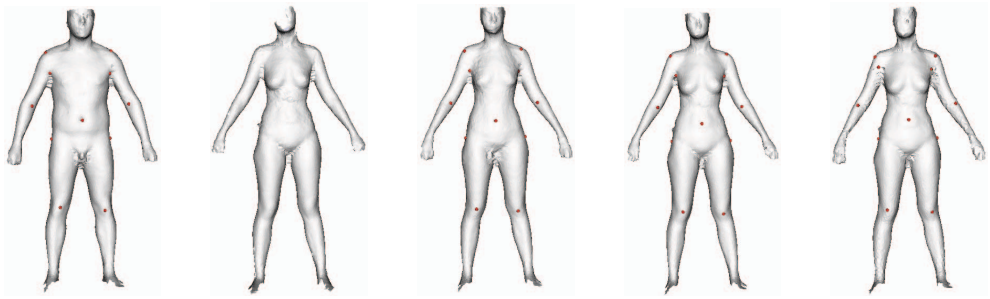

(a) (b) (c) (d) (e)

Fig. 4: Validation of the correspondences, displayed by an example. The source and target surface are displayed in Fig. 4a and Fig. 4b respectively. Fig. 4c shows the annotations on the result of RN-ICP-T and Fig. 4d for the result of RNM-ICP-T. Fig. 4e is the result of N-ICP-A.

better that the source surface migrates slowly to the target surface to reduce the chance on errors. Once a vertex has migrated to the wrong corresponding point, this fault is less likely to be repaired. The more similar the surfaces, the more elastic the source surface can behave. In any case, it is best to end with a small stiffness value close to 5.

In Fig. 5, the influence of the stiffness value is tested on 10 clavicula surfaces. The RNM-ICP-T algorithm ran from a start value of 100 to an end-value $\in [0, 100]$, with a step size of 5. The algorithm also ran from a start value $\in [0, 100]$ to an end value of 0.

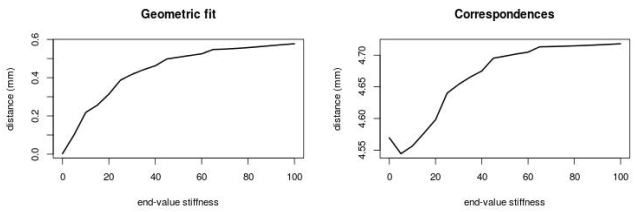

(a) (b)

Fig. 5: Evaluation of the influence of the end stiffness value, tested on 10 clavicula surfaces.

It is clear that it is best to end with a small stiffness value. From Fig. 5b, it can be obeserved that a stiffness value of 0 gives a worse result on correspondences than a value of 5. This is because the vertices have too much freedom to migrate to an inaccurate position, due to drift of the vertices because there are no restrictions. On the other hand, ending with a stiffness of 0 gives the best results on geometric fit. For the start stiffness value has little influence on the results, but a starting with a low stiffness value (less than 20) results in too much freedom of movement and a high stiffness value (more than 80) leads to a registration that is too rigid. From tests it turned out that a start value of 50 gives acceptable good results on correspondence and geometric fit for all types of surfaces.

F. Evaluation of the Timing

The execution time of the algorithm depends on the number of vertices, because this determines how many times there must be searched for corresponding points and the size of the linear system.

A test is performed on 10 surfaces, registered by the three techniques for 50 iterations. The results are shown in Table III.

	N-ICP-A	**RN-ICP-T**	**RNM-ICP-T**
head	578 ± 102	$\mathbf{14 \pm 4}$	16 ± 4
body	-	$\mathbf{5 \pm 1}$	6 ± 1
ear	-	166 ± 62	$\mathbf{127 \pm 30}$
clavicula	-	$\mathbf{12 \pm 2}$	15 ± 2

TABLE III: Run times of the algorithm (min)

Amberg's algorithm has the largest calculation time. The most time consuming parts of the RN-ICP-T and RNM-ICP-T algorithms are the solving of the linear system and the determination of the corresponding points. Solving the linear system takes about $1/3$ of the total time of an iteration. The determination of the corresponding points takes about $1/3$ of the time for as well the rigid as elastic registration. For Amberg's algorithm, the solving of the linear system takes most of the time, about 99% of the total time of an iteration. In our implementation, this is because the number of unknowns is four times larger relative to the one used in this presented framework. This leads to a factor 40 increment in time, compared to the proposed algorithms in this paper.

G. Influence of the Number of Iterations

For the previous tests, the RN-ICP-T, RNM-ICP-T and N-ICP-A algorithms ran 50 iterations. The number of iterations determines how fast the stiffness decreases and the weight factor α increases, because these parameters evolve linearly to a fixed end value. During the first iterations, the registration is more global because of the low weight factor α and the small number of eigenmodes. At the end it becomes elastic and the deformation is more refined.

When the number of iterations is small, e.g. less than 30, there is not much time to obtain a good rough and fine registration. This may lead to an inexact registration. On the other hand, by setting the number of iterations too high the algorithm will take too long without improvement with respect

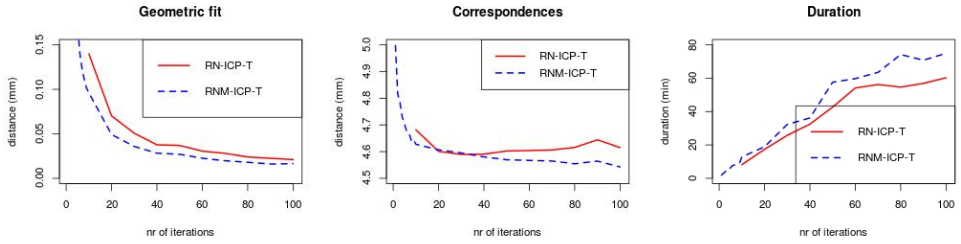

(a) (b) (c)

Fig. 6: The more iterations, the smaller the geometric error. It is seen in Fig. 6a that this applies to both RN-ICP-T and RNM-ICP-T. Fig. 6b shows that the correspondence error decreases more for RNM-ICP-T than for RN-ICP-T. The execution time of both algorithms increases linearly, as seen in Fig. 6c.

to less iterations. The number of iterations will depend on the desired precision of the surface registration.

Tests are performed on registration of 10 surfaces of the human head. Each surface is registered by 10 to 100 iterations, with a step size of 10.

For RN-ICP-T, the number of iteration only has a significant influence on the geometric fit and the execution time. There is no improvement on correspondences, while the geometric fit gets better. When registering with a shape model, the correspondences also improve over the iterations. These factors must be taken into account when choosing the number of iterations. For our applications, 50 iterations is sufficient.

IV. Conclusion

In this paper, two new techniques for surface registration were described. They proved to score well on geometric fit, correspondences, and duration, compared to the N-ICP-A algorithm of Amberg. Another advantage over Amberg's algorithm is that the proposed algorithms run about 40 times faster.

The optimal stiffness value depends on the type of surface, or more specifically the number of triangles and the curvature on the surface. The optimal number of iterations also depends on the type of surface and the application. The more similar the surfaces, the fewer iterations are needed for good correspondences and a good geometric fit. For the tests in this paper, all surfaces are resampled to $10,000$ vertices, which makes that all surfaces could be registered with the same start and end stiffness value.

The choice of the number of iterations depends on the desired accuracy of the results. More iterations will yield improved results on correspondence and geometric fit, but the execution time will increase. The tests show that 50 iterations gives good results within an acceptable time frame for each class of surfaces considered in this paper.

Acknowledgment

The authors would like to thank Amit Bernat M.D. for the clavicula scans and Philips for the ear scans.

References

[1] Yingjie Wang, Chin-Seng Chua, and Yeong-Khing Ho. Facial feature detection and face recognition from 2D and 3D images. *Pattern Recognition Letters*, 23(10):1191–1202, August 2002.

[2] Z. Guo, Y.N. Zhang, Y. Xia, Z.G. Lin, Y.Y. Fan, and D.D. Feng. Multi-Pose 3D Face Recognition Based on 2D Sparse Representation. *JVCIR*, 24(2):117-126, February 2013.

[3] Guoyan Zheng, Sebastian Gollmer, Steffen Schumann, Xiao Dong, Thomas Feilkas, and Miguel A. Gonzlez Ballester. A 2D/3D correspondence building method for reconstruction of a patient-specific 3D bone surface model using point distribution models and calibrated x-ray images. *Medical Image Analysis*, 13(6):883–899, December 2009.

[4] Lijing Wang and Xueli He. Model Reconstruction of Human Buttocks and the Shape Clustering. *DHM 2013*, 8026:245-251, January 2013.

[5] Alan Brunton, Augusto Salazar, Timo Bolkart, and Stefanie Wuhrer. Review and comparative analysis of statistical shape spaces of 3D data. arXiv e-print 1209.6491, September 2012.

[6] Peter R.M. Jones and Marc Rioux Three-dimensional Surface Anthropometry: Applications to the Human Body. *Optics and Lasers in Engineering*, 89–117, September 1997.

[7] Hasler, N., Stoll, C., Sunkel, M., Rosenhahn, B., Seidel, H.-P. A statistical model of human pose and body shape. Comput. *Graph. Forum (Special Issue of Eurographics 2008)*, 2(28), 2009.

[8] T.F. Cootes, C.J. Taylor, D.H. Cooper, and J. Graham. Active shape models-their training and application. *Computer Vision and Image Understanding*, 61(1):38–59, January 1995.

[9] Brett Allen, Brian Curless, and Zoran Popovi. The space of human body shapes: reconstruction and parameterization from range scans. *ACM Trans. Graph.*, 22(3):587594, July 2003.

[10] Toon Huysmans and Jan Sijbers. Method for mapping tubular surfaces to a cylinder, 2010. G06T 17/20 (2006.01), A61B 1/00 (2006.01), no. PCT/EP2010/057882, December 2010.

[11] Toon Huysmans, Jan Sijbers, and Brigitte Verdonk. Automatic construction of correspondences for tubular surfaces. *IEEE Transactions on Pattern Analysis and Machine Intelligence*, 32(4):636–651, April 2010.

[12] Chris Maes, Thomas Fabry, Johannes Keustermans, Dirk Smeets, Paul Suetens, and Dirk Vandermeulen. Feature detection on 3D face surfaces for pose normalization and recognition. *BTAS '10, IEEE Int. Conf. on Biometrics: Theory, Applications and Systems*, 1–6, September 2010.

[13] David G. Lowe. Distinctive image features from scale-invariant keypoints. *International Journal of Computer Vision*, 60(2):91–110, November 2004.

[14] Brian Amberg, Sami Romdhani, and Thomas Vetter. Optimal step nonrigid ICP algorithms for surface registration. *CVPR'07*, June 2007.

[15] Heimann, Tobias and Meinzer, Hans-Peter. Statistical shape models for 3D medical image segmentation: A review. *Medical Image Analysis*, 543–563, August 2009.